

# Semi-inclusive electroproduction of hidden-charm and double-charm hadronic molecules

Pan-Pan Shi<sup>1,2,\*</sup>, Feng-Kun Guo<sup>1,2,†</sup> and Zhi Yang<sup>3,‡</sup>

<sup>1</sup>CAS Key Laboratory of Theoretical Physics, Institute of Theoretical Physics, Chinese Academy of Sciences, Beijing 100190, China

<sup>2</sup>School of Physical Sciences, University of Chinese Academy of Sciences, Beijing 100049, China

<sup>3</sup>School of Physics, University of Electronic Science and Technology of China, Chengdu 610054, China



(Received 10 August 2022; accepted 28 November 2022; published 27 December 2022)

The semi-inclusive electroproduction of exotic hadrons, including the  $T_{cc}$ ,  $P_{cs}$ , and hidden-charm baryon-antibaryon states, is explored under the assumption that they are  $S$ -wave hadronic molecules of a pair of charmed hadrons. We employ the Monte Carlo event generator Pythia to produce the hadron pairs and then bind them together to form hadronic molecules. With the use of such a production mechanism, the semi-inclusive electroproduction rates are estimated at the order-of-magnitude level. Our results indicate that a larger number of  $P_{cs}$  states and  $\Lambda_c \bar{\Lambda}_c$  molecules can be produced at the proposed electron-ion colliders in China (EicC) and the US (EIC). The results also suggest that the  $T_{cc}$  states and other hidden-charm baryon-antibaryon states can be searched for at EIC. Besides, the potential 24-GeV upgrade of the Continuous Beam Accelerator Facility at the Thomas Jefferson National Accelerator Facility can play an important role in the search for the hidden-charm tetraquark and pentaquark states due to its high luminosity.

DOI: [10.1103/PhysRevD.106.114026](https://doi.org/10.1103/PhysRevD.106.114026)

## I. INTRODUCTION

In the last two decades, a number of hadron structures have been observed in various high-energy experiments, such as BESIII [1], LHCb [2], and Belle [3]. Many of these structures possess properties incompatible with the predictions of the traditional quark model for quark-antiquark mesons and three-quark baryons, and therefore are excellent candidates for the so-called exotic hadrons. These structures have been studied extensively with different models, but debates about their nature still exist (for recent reviews, see Refs. [4–13]).

So far, most of the exotic states have been observed at hadron-hadron and electron-positron collisions. To understand the nature of the exotic states, other production processes have been proposed to search for these states. Notably, photoproduction or leptonproduction processes have the advantage that the possible resonant signals are free of triangle singularities (for a review, see Ref. [12]).

Pioneering work in the search for exotic hadrons in photoproduction processes has been done by the COMPASS and GlueX collaborations. The COMPASS Collaboration searched for  $Z_c(3900)^\pm$  in the  $J/\psi\pi^\pm$  invariant-mass distribution, but there was no signal [14]. Later, the COMPASS Collaboration observed a peak around 3.86 GeV in the  $J/\psi\pi^+\pi^-$  invariant-mass distribution with a  $4.1\sigma$  statistical significance— $\tilde{X}(3872)$ —in muoproduction processes [15], and the measured  $\pi^+\pi^-$  invariant-mass distribution indicates a negative  $C$  parity for this structure. The GlueX Collaboration found no evidence of hidden-charm pentaquark  $P_c$  states in near-threshold  $J/\psi$  exclusive photoproduction off the proton in Hall D at the Thomas Jefferson National Accelerator Facility (JLab) and set model-dependent upper limits (using a vector-meson-dominance model) for the branching fractions  $\text{Br}[P_c^+ \rightarrow J/\psi p]$  [16].

The proposed electron-ion collider in China (EicC) [17], the Electron-Ion Collider in the US (EIC) [18], and the potential 24-GeV upgrade of the Continuous Beam Accelerator Facility (CEBAF) at JLab [19] provide new opportunities to search for exotic hadron structures and study the nature of such states. The center-of-mass (c.m.) energies at EicC and EIC are much higher than the thresholds of charmed hadron pairs, and thus they permit semi-inclusive electroproduction of hidden-charm (and even double-charm) exotic states. For CEBAF (24 GeV), the c.m. energy of the electron-proton system with a

\*shipanpan@itp.ac.cn

†fkguo@itp.ac.cn

‡zhiyang@uestc.edu.cn

Published by the American Physical Society under the terms of the [Creative Commons Attribution 4.0 International license](https://creativecommons.org/licenses/by/4.0/). Further distribution of this work must maintain attribution to the author(s) and the published article's title, journal citation, and DOI. Funded by SCOAP<sup>3</sup>.

TABLE I. Energy configurations and luminosities for EicC, EIC, and the proposed 24 GeV upgrade of CEBAF. The integrated luminosities correspond to about 1 year of operation.

	EicC [17]	EIC [18]	CEBAF (24 GeV) [19]
$e$ (GeV)	3.5	18	24
$p$ (GeV)	20	275	0
Luminosity ( $\text{cm}^{-2} \text{s}^{-1}$ )	$2 \times 10^{33}$	$10^{34}$	$10^{36}$
Integrated luminosity ( $\text{fb}^{-1}$ )	60	300	$3 \times 10^4$

24 GeV electron beam hitting the proton target is about 6.7 GeV and thus much lower than that at EicC and EIC; yet, its luminosity is much higher. The energy configurations and luminosities of these facilities are listed in Table I.

Many works have estimated the cross sections for the exclusive photoproduction of the hidden-charm pentaquark states [20–32] and hidden-charm tetraquark states [33–38] with the vector-meson dominance model, which assumes that the photon emitted from the electron converts into a  $J/\psi$  which then interacts with the proton to produce the hidden-charm states. Yet, since the production of a heavy quarkonium, such as  $J/\psi$ , in high-energy reactions requires the heavy quark and antiquark pair to be confined in a small phase space, its production rate is much lower than that of a pair of open-charm hadrons. In view of this, the open-charm hadron pair might be a crucial component in producing exotic hadrons with hidden-charm. In particular, in Ref. [39] it was pointed out that the total cross section for the near-threshold photoproduction of  $J/\psi$  in  $\gamma J/\psi \rightarrow J/\psi p$  measured by GlueX is consistent with assuming that the reaction is dominated by the  $\Lambda_c \bar{D}^{(*)}$  channels through  $\gamma J/\psi \rightarrow \Lambda_c \bar{D}^{(*)} \rightarrow J/\psi p$ . Furthermore, the results for the heavy vector quarkonia, calculated by solving the Dyson-Schwinger equation, are incompatible with the assumption of the vector-meson-dominance model in the electroproduction process [40]. Therefore, it is necessary to explore the photoproduction of exotic states with other methods.

Based on the hadronic molecular picture, the semi-inclusive leptonproduction rates of the hidden-charm hadrons at COMPASS, EicC, and EIC were estimated in Ref. [41]. The considered production mechanism is such that the charmed hadron pairs are semi-inclusively generated with the use of a Monte Carlo (MC) event generator and then bound together to form hadronic molecules through the final-state interaction (FSI) [42–44]. This mechanism has been employed to estimate the cross sections at the order-of-magnitude level for the production of  $X(3872)$  [45–47], the spin partner and bottom analogues of  $X(3872)$  [44], the charm-strange hadronic molecules [43], the charged charmonium-like and bottomonium-like states [48], the  $P_c$  states [49], and dionium ( $D^+ D^-$

hadronic atom) [50]. The so-obtained cross sections for the production of  $X(3872)$  [8] at hadron colliders are in line with the measurements at CDF [51] and CMS [52].

In this work, we employ the same mechanism to estimate the cross sections for the semi-inclusive electroproduction of the double-charm  $T_{cc}$  states, hidden-charm  $P_{cs}$  states, and hidden-charm baryon-antibaryon states at EicC and EIC, which have not been given before, and the semi-inclusive electroproduction rates of  $X(3872)$ ,  $Z_c(3900)^{0(+)}$ , the  $P_c$  states, and  $P_{cs}(4459)$  at JLab for the first time.<sup>1</sup> Among the exotic states discussed in this work,  $P_c(4312)$ ,  $P_c(4440)$ ,  $P_c(4457)$ ,  $P_{cs}(4459)$ , and  $T_{cc}^+$  were observed by the LHCb Collaboration [53–56],  $X(3872)$  was first reported by the Belle Collaboration [57],  $Z_c(3900)^+$  was discovered by the BESIII and Belle Collaborations [58,59], and  $Z_c(3900)^0$  was observed by the BESIII Collaboration [60]. The rest of the states are predicted in the hadronic molecular picture; see Refs. [61,62] for a survey of the spectrum of hidden-charm and double-charm hadronic molecules.

This paper is organized as follows. In Sec. II we introduce the semi-inclusive electroproduction mechanism of hadronic molecules. Our numerical results and the production rates for the exotic states at EicC, EIC, and the 24 GeV upgrade of CEBAF are presented in Sec. III. We briefly summarize our work in Sec. IV. The Appendix contains the derivation of the production cross section of the spin-3/2 molecule, which is composed of a baryon and a vector meson.

## II. SEMI-INCLUSIVE PRODUCTION MECHANISM

As shown in Fig. 1, the mechanism for the semi-inclusive electroproduction of a hadronic molecule involves a virtual photon, radiated by the electron, interacting with the proton to produce the hadron pair  $HH'$  and other particles denoted by “all” [41]; then, the  $HH'$  pair is bound together to form a hadronic molecule through the FSI. Therefore, the amplitude of the semi-inclusive production of the hadronic molecule  $X$  can be factorized into a short-distance part and a long-distance part [43,44,46,63],<sup>2</sup>

<sup>1</sup>The cross sections for the production of the  $P_c$  states are significantly small due to the low c.m. energy (up to about 4.8 GeV) at the running JLab experiments. In this work, we only discuss the possible upgrade of CEBAF with an electron energy of 24 GeV.

<sup>2</sup>In the framework used here, the long-distance part refers to the formation of hadronic molecules from the hadron-pair interactions, and thus the momentum scale is roughly the binding momentum  $\kappa = \sqrt{2\mu B}$ , where  $\mu$  is the reduced mass of the two-body system and  $B$  refers to the binding energy. In this sense, momentum scales that are much larger than  $\kappa$  qualify as short-distance scales. The production of charmed hadrons through partonic interactions is thus a short-distance process.

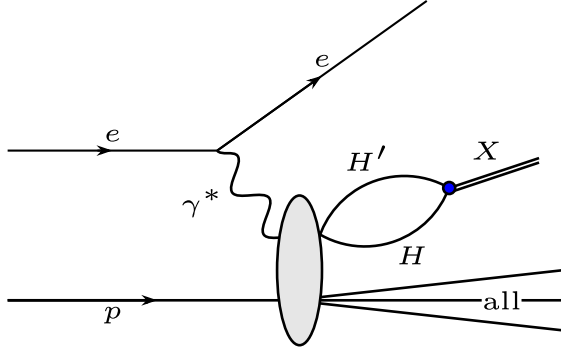


FIG. 1. Semi-inclusive electroproduction of the  $HH'$  hadronic molecule  $X$  in  $ep$  collisions. The other particles produced in this process are generally denoted by "all."

$$\mathcal{M}[X + \text{all}] = \mathcal{M}[HH' + \text{all}] \cdot G \cdot T_X, \quad (1)$$

where  $T_X$  denotes the amplitude for the long-distance process of fusing the  $HH'$  pair into the hadronic molecule  $X$ , which can be approximated by the effective coupling constant for  $X$  to its constituents in the case of loosely bound hadronic molecules, and the rest is the short-distance part.  $\mathcal{M}[HH' + \text{all}]$  denotes the amplitude for the short-distance process  $ep \rightarrow HH' + \text{all}$ , and  $G$  denotes the Green's function of the  $HH'$  pair, which is ultraviolet divergent and the divergence can be absorbed by  $\mathcal{M}[HH' + \text{all}]$  [63].

For the production process  $ep \rightarrow HH' + \text{all}$ , the semi-inclusive production of  $HH'$  at short distances may be simulated using the MC event generator Pythia [64]. The most important hard scattering process is  $\gamma g \rightarrow c\bar{c}$  for the production of charm-hadron pairs considered here. In our explicit realization, we choose the hard process in Pythia to generate the partonic events and then the  $HH'$  events can be obtained after the hadronization. The general differential cross section for the inclusive production of  $HH'$  in the MC event generator is

$$\begin{aligned} d\sigma[HH'(k)]_{\text{MC}} \\ = K_{HH'} \frac{1}{\text{flux}} \sum_{\text{all}} \int d\phi_{HH'+\text{all}} |\mathcal{M}[HH' + \text{all}]|^2 \frac{d^3k}{(2\pi)^3 2\mu}, \end{aligned} \quad (2)$$

where  $k$  and  $\mu$  are the three-momentum in the c.m. frame and the reduced mass of the  $HH'$  system, respectively. The difference between the MC simulation and the experimental data is amended by an overall factor  $K_{HH'}$ . To estimate the cross sections for the semi-inclusive electroproduction of hadronic molecules at the order-of-magnitude level, we roughly set  $K_{HH'} \simeq 1$ . The total cross section for the semi-inclusive production of a hadronic molecule  $X$  can be derived from Eqs. (1) and (2),

$$\sigma[X + \text{all}] \simeq \frac{\mathcal{N}}{4m_H m_{H'}} |GT_X|^2 \left( \frac{d\sigma[HH' + \text{all}]}{dk} \right)_{\text{MC}} \frac{4\pi^2 \mu}{k^2}, \quad (3)$$

where  $m_H(m_{H'})$  is the mass of  $H(H')$ ,  $\mathcal{N} = 2/3$  for the production of the  $\Sigma_c \bar{D}^*$  and  $\Xi_c \bar{D}^*$  molecular states with quantum numbers  $J^P = 3/2^-$  (see the Appendix), and  $\mathcal{N} = 1$  for the other hadronic molecules considered in this work. Here we neglect the scattering between  $H(H')$  and other final-state particles. Then, the differential cross section for  $HH'$  production in the MC event generator is

$$\left( \frac{d\sigma[HH' + \text{all}]}{dk} \right)_{\text{MC}} \propto k^2. \quad (4)$$

The Green's function  $G$  in Eq. (3) is ultraviolet divergent and can be regularized by a Gaussian regulator as [65]

$$G(E, \Lambda) = -\frac{\mu}{\pi^2} \left\{ \sqrt{2\pi} \frac{\Lambda}{4} + \frac{k\pi}{2} e^{-2k^2/\Lambda^2} \left[ i - \text{erfi} \left( \frac{\sqrt{2}k}{\Lambda} \right) \right] \right\}, \quad (5)$$

where the three-momentum  $k$  is related to the energy  $E$  of the  $HH'$  pair, i.e.,  $k^2 = 2\mu(E - m_H - m_{H'})$ , and  $\text{erfi}(z) = 2/\sqrt{\pi} \int_0^z e^{t^2} dt$  is the imaginary error function. The short-distance amplitude for producing the  $HH'$  pair in Eq. (1) should scale as  $\Lambda^{-1}$  so as to absorb the leading  $\Lambda$  dependence in Eq. (5) [63]. Here, since we have taken the short-distance amplitude to be fixed from the MC event generator, which does not have a  $\Lambda$  dependence, we choose the cutoff  $\Lambda$  to be in the reasonable range 0.5–1.0 GeV as an estimate [61,66–68].

For all of the considered hadronic molecules, the mass is close to the threshold of  $HH'$  which couples to the hadronic molecule in an  $S$  wave. Thus, the amplitude  $T_X$  in Eq. (3) can be approximated by an effective coupling constant  $g_{\text{eff}}$ . The coupling constant  $g_{\text{eff}}$  can be extracted from the  $T$  matrix for the low-energy scattering process  $HH' \rightarrow HH'$ ,

$$g_{\text{eff}}^2 = \lim_{E \rightarrow E_0} (E^2 - E_0^2) T(E), \quad (6)$$

where  $E_0$  is the pole position in the complex  $E$  plane of the  $HH'$  scattering  $T$  matrix. We have  $E_0 = M_X$  for a bound or virtual state (with the pole on the first or second Riemann sheet) and  $E_0 = M_X - i\Gamma/2$  for a resonance (with the pole on the second Riemann sheet). Here  $M_X$  and  $\Gamma$  are the mass and decay width of the hadronic molecule  $X$ , respectively. Near the threshold, we only consider a constant contact term as the interaction kernel  $V$  for the scattering process

$HH' \rightarrow HH'$ . Then, the  $T$  matrix for the scattering of  $HH' \rightarrow HH'$  can be calculated by solving the Lippmann-Schwinger equation,

$$T(E) = \frac{V}{1 - VG(E, \Lambda)}. \quad (7)$$

Poles of the  $T$  matrix on the first or second Riemann sheet of the complex  $E$  plane satisfy the equation  $\det[1 - VG(E_0, \Lambda)] = 0$ . Note that in the evaluation of the effective coupling (6),  $T(E)$  should take a value according to the specific Riemann sheet where the pole is located.

We consider isospin-breaking effects for  $X(3872)$  by considering both the  $D^0\bar{D}^{0*} + \text{c.c.}$  and  $D^+D^{*-} + \text{c.c.}$  channels, and the  $V$  matrix is

$$V = \frac{1}{2} \begin{pmatrix} C_0 + C_1 & C_0 - C_1 \\ C_0 - C_1 & C_0 + C_1 \end{pmatrix}, \quad (8)$$

where  $C_0$  and  $C_1$  are the low-energy constants for the isoscalar and isovector  $D\bar{D}^* + \text{c.c.}$  channels, respectively. The two low-energy constants can be solved using the  $X(3872)$  mass [69] and the isospin-violation ratio [70] for the  $X(3872)$  decays to  $J/\psi\pi^+\pi^-$  and  $J/\psi\pi^+\pi^0\pi^-$  as inputs [71]. We also take the contact term as the potential for  $Z_c(3900)^0$  and  $Z_c(3900)^+$ , where the values of the low-energy constants were fixed in Ref. [68] from fitting to the BESIII data on  $Z_{cs}(3985)$  [72]. For the other exotic states discussed in this work, we neglect the isospin-breaking effects and extract the coupling constants from the single-channel  $T$  matrix.

### III. NUMERICAL RESULTS

The production mechanism discussed in Sec. II is applied to estimate the cross sections for the semi-inclusive electroproduction of hadronic molecules. We simulate the  $ep$  collisions at EicC, EIC, and CEBAF (24 GeV) with the MC event generator Pythia [64] and get the differential cross sections for the semi-inclusive production of the  $HH'$  pair,  $(d\sigma[HH' + \text{all}]/dk)_{\text{MC}}$ . As discussed in Eq. (4), the differential cross section for producing the  $HH'$  pair is proportional to  $k^2$  in the small-momentum region (in this work, we choose  $|k| < 350$  MeV). For instance, the differential MC cross sections for  $\Xi_c^0\bar{D}^{*0}$  pair production at EicC and EIC and in fixed-target  $ep$  collisions,<sup>3</sup> as shown in Fig. 2, are exactly proportional to  $k^2$ .

<sup>3</sup>The c.m. collision energy for the 24 GeV upgrade of CEBAF [19] is lower than 10 GeV, the lower limit for the use of Pythia [64]. To estimate the cross sections, we calculate the cross sections at the electron energies  $E_e = 60, 80, 100$ , and 150 GeV, and then extrapolate the results to  $E_e = 24$  GeV.

For the long-distance part, as discussed above, we use the cutoff-dependence formula in Eq. (3) with the cutoff  $\Lambda \in [0.5, 1.0]$  GeV for an order-of-magnitude estimate of the cross section. To extract the effective coupling  $g_{\text{eff}}$ , the masses and quantum numbers of the hadronic molecules in Tables II and III are fixed to experimental observations, whenever possible, and theoretical predictions. For the  $T_{cc}$  states, the mass of  $T_{cc}^+$  is set by the central value reported by the LHCb Collaboration [55,56], while the  $T_{cc}^*$  mass is set to the theoretical prediction in Ref. [73].  $P_{cs}(4459)$ , which was observed by the LHCb Collaboration [54], might be a  $\Xi_c\bar{D}^*$  bound state with  $J^P = 1/2^-$  or  $3/2^-$  or the signal of both states [61,74–77], and thus we estimate its production rates with both  $J^P = 1/2^-$  and  $3/2^-$ . In Ref. [61], more than 200 hidden-charm hadronic molecules were predicted. In addition to those whose production rates were estimated in Ref. [41], we consider here the  $\Xi_c\bar{D}$  molecule and a set of hidden-charm baryon-antibaryon molecules, composed of  $\Lambda_c\bar{\Lambda}_c$ ,  $\Sigma_c\bar{\Sigma}_c$ ,  $\Xi_c\bar{\Xi}_c$ ,  $\Lambda_c\bar{\Sigma}_c$ ,  $\Lambda_c\bar{\Xi}_c$ , and  $\Xi_c\bar{\Sigma}_c$ . Among these states predicted in Ref. [61], the  $\Xi_c\bar{\Xi}_c$  molecule with  $IJ^{PC} = 10^{-+}$  is a virtual state; the  $\Xi_c\bar{D}$  and  $\Lambda_c\bar{\Xi}_c$  molecules are virtual states when  $\Lambda = 0.5$  GeV, while they are bound states when  $\Lambda = 1$  GeV; the other states are bound states. Following Refs. [78–80], we assign  $P_c(4312)$  and the narrow  $P_c(4380)$  [79] as the  $\Sigma_c\bar{D}$  molecule with  $J^P = 1/2^-$  and the  $\Sigma_c^*\bar{D}$  molecule with  $J^P = 1/2^-$ , respectively, and  $P_c(4440)$  and  $P_c(4457)$  as the  $\Sigma_c\bar{D}^*$  molecules with  $J^P = 3/2^-$  and  $1/2^-$ . Following Ref. [41], we use the  $P_c$  masses from scheme II in Ref. [79] as inputs to extract the effective coupling constants  $g_{\text{eff}}$ .

We estimate the cross sections for the production of the molecules, as shown in Table II, at EicC and EIC with the energy configurations in Table I. Our results show that the cross sections at EIC are roughly 1 order of magnitude larger than that at EicC for producing hidden-charm hadronic molecules, which are in line with the estimates in Ref. [41]. However, as shown in Table II, this difference increases to 2 orders of magnitude for the  $T_{cc}$  states. Such a difference is caused by the different charm numbers between the  $T_{cc}$  states and hidden-charm states. In the processes for the production of the  $T_{cc}$  states, at least two charm quarks and two anticharm quarks should be generated in  $ep$  collisions. Comparing with the production of the hidden-charm exotic states, higher c.m. collision energies are required to efficiently produce the  $T_{cc}$  states. With the energy configurations listed in Table I, the c.m. collision energy for EicC is about 17 GeV, which is smaller than that of EIC (about 141 GeV), so the cross sections for producing the  $T_{cc}$  states are reasonably small.

As listed in Table II, the cross sections for the double-charm states,  $T_{cc}^+$  and  $T_{cc}^*$ , are at the level of 1 fb and



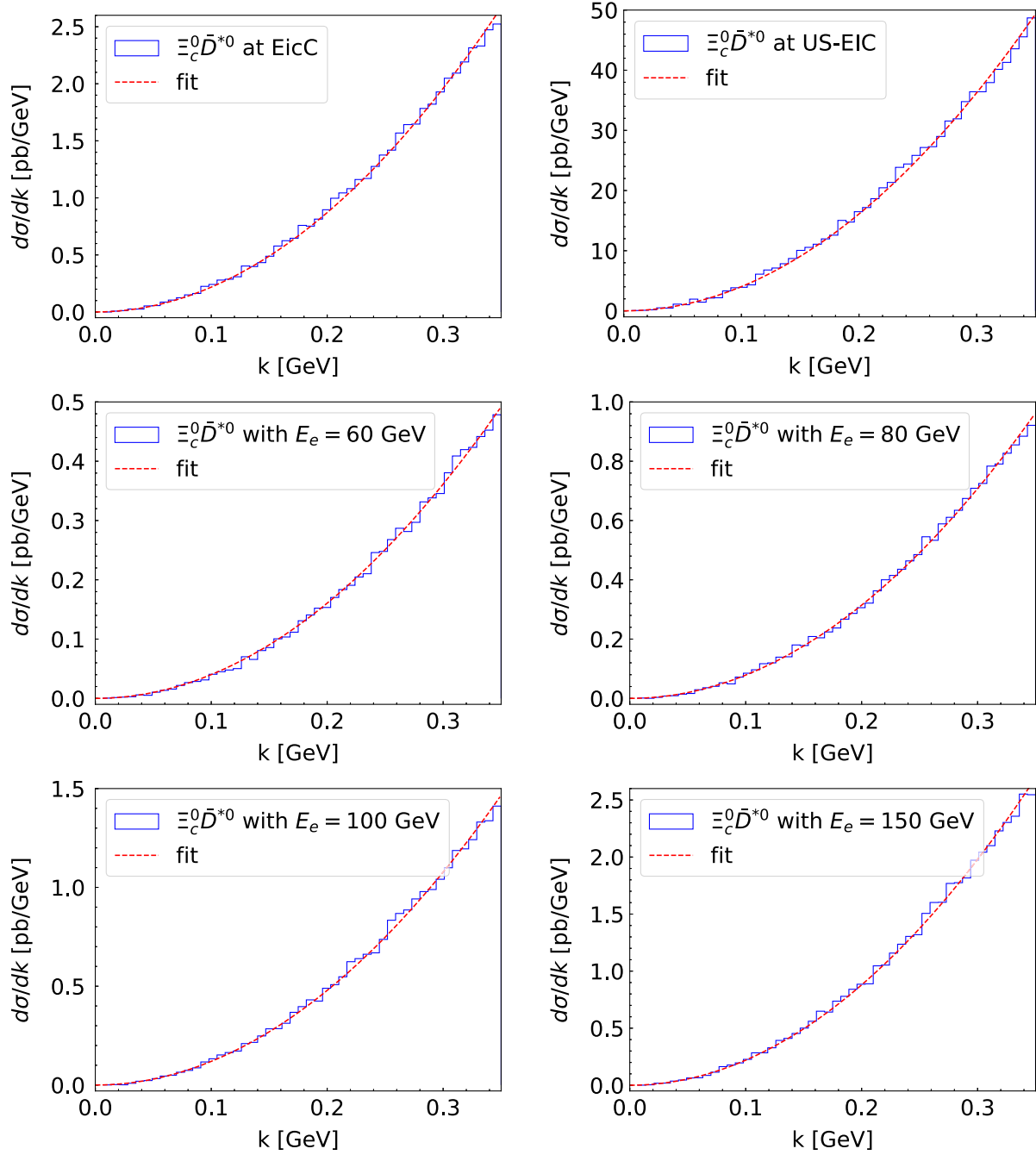


FIG. 2. Differential cross sections  $d\sigma/dk$  for the production of  $\Xi_c^0 \bar{D}^{*0}$  in  $ep$  collisions. The histograms are generated using Pythia and the dashed curves are from fits using  $d\sigma/dk \propto k^2$ . In the lower four plots, the proton is at rest and  $E_e$  denotes the energy of the electron beam.

0.1 pb for EicC and EIC, respectively. Thus, the estimated numbers of  $T_{cc}^+$  events are 18–72 at EicC and  $3 \times 10^4$ – $1.5 \times 10^5$  at EIC with the integral luminosities listed in Table I. In particular, our estimate for the  $T_{cc}^+$  event number is significantly smaller than the number of double-charm baryon  $\Xi_{cc}$  events (about  $4.0 \times 10^5$  in a year) estimated in Ref. [17]. Given that the event numbers of  $T_{cc}^+$  [56] and  $\Xi_{cc}^+$  [82] observed by the

LHCb Collaboration are of the same order of magnitude,<sup>4</sup> investigations are needed to understand the large difference. The cross sections for the  $P_{cs}$  states are around

<sup>4</sup>The event number for  $\Xi_{cc}^{++} \rightarrow \Lambda_c^+ (\rightarrow p K^- \pi^+) K^- \pi^+ \pi^+$  is  $313 \pm 33$  with an integrated luminosity of  $1.7 \text{ fb}^{-1}$  [82]; the event number for  $T_{cc}^+ \rightarrow D^0 (\rightarrow K^- \pi^+) \bar{D}^0 (\rightarrow K^+ \pi^-) \pi^+$  is  $117 \pm 16$  with an integrated luminosity of  $9 \text{ fb}^{-1}$  [56].

TABLE II. Order-of-magnitude estimates of the cross sections (in units of pb) for  $ep \rightarrow X + \text{all}$  at EicC and EIC, where  $X$  denotes one of the two  $T_{cc}$  states, three  $P_{cs}$  states, and some hidden-charm baryon-antibaryon molecules. The quantum numbers for those states are listed in the third column. The binding energies, defined as  $m_1 + m_2 - M$  where  $m_{1,2}$  are the masses of the constituents and  $M$  is the mass of the hadronic molecule, are listed in the fourth column. The results outside (inside) parentheses denote the cross sections with  $\Lambda = 0.5$  GeV (1.0 GeV).

	Constituents	$IJ^{P(C)}$	Binding energy (MeV)	EicC (pb)	EIC (pb)
$T_{cc}^+$	$DD^*$	$01^+$	0.273 [55,56]	$0.3 \times 10^{-3} (1.2 \times 10^{-3})$	0.1 (0.5)
$T_{cc}^*$	$D^*D^*$	$01^+$	0.503 [73]	$0.2 \times 10^{-3} (1.0 \times 10^{-3})$	0.1 (0.4)
$P_{cs}$	$\Xi_c \bar{D}$	$0\frac{1}{2}^-$	0.3 (3.53) [61]	0.1 (1.6)	1.8 (30)
$P_{cs}$	$\Xi_c \bar{D}^*$	$0\frac{1}{2}^-$	18.83 [81]	0.1 (0.5)	1.3 (8.8)
$P_{cs}$	$\Xi_c \bar{D}^*$	$0\frac{3}{2}^-$	18.83 [81]	0.1 (0.9)	2.6 (18)
	$\Lambda_c \bar{\Lambda}_c$	$00^{-+}$	1.98 (33.8) [61]	0.3 (3.0)	9.6 (110)
	$\Sigma_c \bar{\Sigma}_c$	$00^{-+}$	11.1 (60.8) [61]	$0.7 \times 10^{-3} (5.2 \times 10^{-3})$	0.04 (0.29)
	$\Sigma_c \bar{\Sigma}_c$	$10^{-+}$	8.28 (53) [61]	$0.7 \times 10^{-3} (5.3 \times 10^{-3})$	0.04 (0.29)
	$\Xi_c \bar{\Xi}_c$	$00^{-+}$	4.72 (42.2) [61]	$1.4 \times 10^{-3} (1.1 \times 10^{-2})$	0.1 (0.5)
	$\Xi_c \bar{\Xi}_c$	$10^{-+}$	18.2 (0.39) [61]	$0.1 \times 10^{-3} (1.7 \times 10^{-3})$	$3.9 \times 10^{-3} (7.1 \times 10^{-2})$
	$\Lambda_c \bar{\Sigma}_c$	$10^-$	2.19 (33.9) [61]	0.01 (0.12)	0.5 (5.5)
	$\Lambda_c \bar{\Xi}_c$	$\frac{1}{2}0^-$	1.29 (8.42) [61]	0.01 (0.14)	0.2 (5.3)
	$\Xi_c \bar{\Sigma}_c$	$\frac{1}{2}0^-$	5.98 (46.4) [61]	$0.8 \times 10^{-3} (7.3 \times 10^{-3})$	0.04 (0.36)

1 pb at EicC and tens of pb at EIC, so that we expect at least  $6 \times 10^3$  and  $3.9 \times 10^5$  events for the  $P_{cs}$  states produced at EicC and EIC, respectively. The estimated cross sections of the  $P_{cs}$  states are of the same order as those of the  $P_c$  states estimated in Ref. [41].

Our results indicate that, at EicC and EIC, the production rates for the  $\Lambda_c \bar{\Lambda}_c$  molecule with quantum numbers  $IJ^{PC} = 00^{-+}$  are significantly larger than those for the other baryon-antibaryon molecules listed in Table II. The events for the  $\Lambda_c \bar{\Lambda}_c$  molecule are about

TABLE III. Order-of-magnitude estimates of the cross sections for  $ep \rightarrow X + \text{all}$  at the proposed 24 GeV upgrade of CEBAF, where  $X$  denotes one of the hidden-charm hadronic molecules,  $X(3872)$ ,  $Z_c(3900)^{0(+)}$ , four  $P_c$  states, and two  $P_{cs}$  states. The results outside (inside) the parentheses are the cross sections estimated with  $\Lambda = 0.5$  GeV (1.0 GeV).

	Constituents	$IJ^{P(C)}$	Binding energy (MeV)	$\sigma_X$ (pb)
$X(3872)$	$D\bar{D}^*$	$01^{++}$	4.15	1.3 (5.5)
$Z_c(3900)^0$	$D\bar{D}^*$	$11^{+-}$	-12.57	22.9 (82.4)
$Z_c(3900)^+$	$D^{*+}\bar{D}^0$	$11^+$	-13.30	16.2 (59.2)
$P_c(4312)$	$\Sigma_c \bar{D}$	$\frac{1}{2}\frac{1}{2}^-$	6.68	0.02 (0.08)
$P_c(4440)^+$	$\Sigma_c \bar{D}^*$	$\frac{1}{2}\frac{3}{2}^-$	21.06	0.01 (0.06)
$P_c(4457)^+$	$\Sigma_c \bar{D}^*$	$\frac{1}{2}\frac{1}{2}^-$	3.06	$3.4 \times 10^{-3} (16.4 \times 10^{-3})$
$P_c(4380)^+$	$\Sigma_c^* \bar{D}$	$\frac{1}{2}\frac{3}{2}^-$	7.18	0.03 (0.15)
$P_{cs}(4459)$	$\Xi_c \bar{D}^*$	$0\frac{3}{2}^-$	18.83	$4.9 \times 10^{-3} (33.2 \times 10^{-3})$
$P_{cs}(4459)$	$\Xi_c \bar{D}^*$	$0\frac{1}{2}^-$	18.83	$2.4 \times 10^{-3} (16.6 \times 10^{-3})$

$2 \times 10^4$ – $2 \times 10^5$  and  $3 \times 10^6$ – $3 \times 10^7$  at EicC and EIC, respectively. Therefore, it is promising to find the  $\Lambda_c \bar{\Lambda}_c$  molecule and study its properties in detail at EicC and EIC. Besides, for the  $\Xi_c \bar{\Xi}_c$  molecule with  $IJ^{PC} = 10^{-+}$ , we expect that about 10–100 and  $1 \times 10^3$ – $2 \times 10^4$  events can be produced at EicC and EIC, respectively, and thus it can be searched for at EIC.

As for CEBAF (24 GeV), because the c.m. collision energy is below the applicable energy range of Pythia, we estimate the cross sections for producing the hidden-charm hadronic molecules at higher electron energies (60, 80, 100, and 150 GeV) and then extrapolate the results to 24 GeV. The extrapolation, as shown in Figs. 3 and 4, is further constrained by requiring the cross section to vanish at the relevant threshold. The so-estimated cross sections for the production of a set of hidden-charm

hadronic molecules at the proposed 24 GeV upgrade of CEBAF are listed in Table III. The cross sections are around 1 pb for producing  $X(3872)$ , and 0.01 pb for producing the  $P_c$  and  $P_{cs}$  states. Although the cross sections at CEBAF (24 GeV) are significantly smaller than those at EicC and EIC, its much higher integrated luminosity listed in Table I still permits a large number of events for certain hidden-charm exotic hadrons to be produced. For instance,  $\mathcal{O}(10^7$ – $10^8)$   $X(3872)$  can be produced through the semi-inclusive processes. Considering the branching fractions  $\text{Br}(X(3872) \rightarrow J/\psi \pi \pi) = (3.8 \pm 1.2)\%$  and  $\text{Br}(J/\psi \rightarrow l^+ l^-) = 12\%$  [83], the event numbers will be  $\mathcal{O}(10^5$ – $10^6)$  for one year of operation. Besides, the cross sections for the  $Z_c$  states are 1 order of magnitude larger than that for  $X(3872)$ , which are compatible with the estimate at EicC and EIC [41].

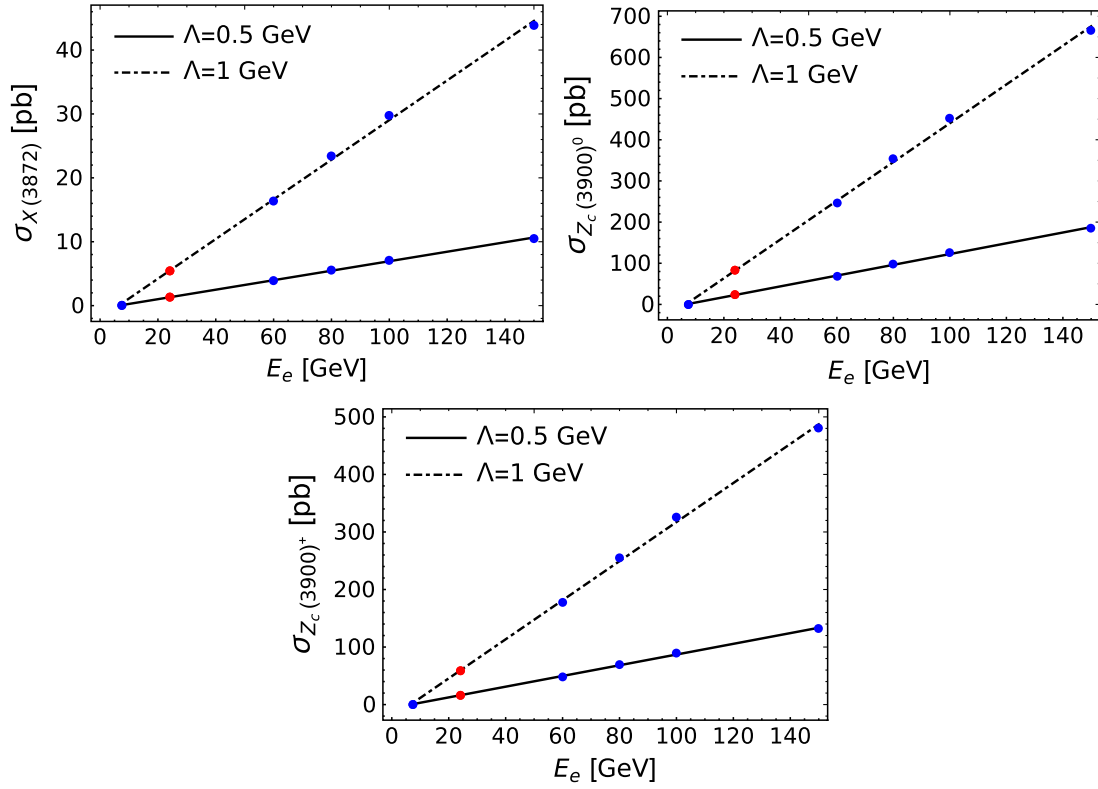


FIG. 3. Semi-inclusive cross sections for producing  $X(3872)$  and  $Z_c(3900)^{0(+)}$  through the  $ep \rightarrow X + \text{all}$  reactions with the proton at rest.  $E_e$  denotes the electron energy in the process, and  $X$  denotes  $X(3872)$  or  $Z_c$ . The blue points represent the cross sections estimated at different electron energies and the red points are the cross sections extrapolated to  $E_e = 24$  GeV.

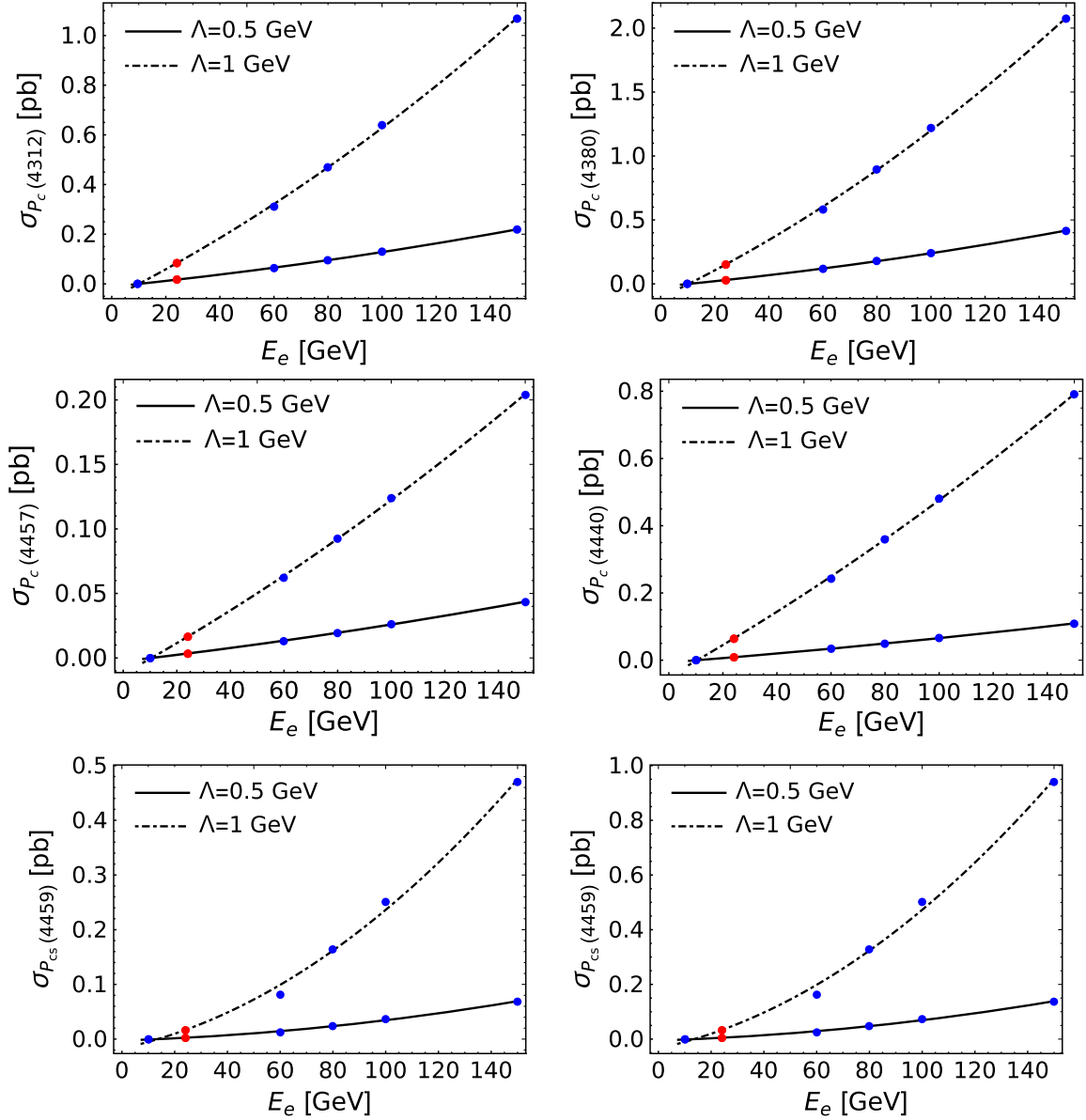


FIG. 4. Semi-inclusive cross sections for producing hidden-charm pentaquarks through the  $ep \rightarrow X + \text{all}$  reactions with the proton at rest.  $E_e$  denotes the electron energy in the process, and  $X$  denotes  $P_c$  or  $P_{cs}$ . The blue points represent the cross sections estimated at different electron energies and the red points are the cross sections extrapolated to  $E_e = 24$  GeV. In the last row, the left and right plots are the results assuming the spin of the  $P_{cs}(4459)$  to be  $1/2$  and  $3/2$ , respectively.

#### IV. SUMMARY

In this work, based on the hadronic molecular picture, we have estimated the semi-inclusive electroproduction rates of the typical multiquark states at EicC, EIC, and the proposed 24 GeV upgrade of CEBAF.

We have employed the MC event generator Pythia to simulate the production of charmed hadron pairs at short distances. Then, the hadron pairs are bound together to form hadronic molecules through FSI at long distances. The production rates for typical tetraquarks, hidden-charm pentaquarks, and hidden-charm baryon-antibaryon molecules were estimated with such a production mechanism at

EicC, EIC, and CEBAF (24 GeV). Since the c.m. energy of CEBAF (24 GeV) is below the applicable energy range of Pythia, we have calculated the production rates with the electron energy at  $E_e = 60, 80, 100$ , and  $150$  GeV and then extrapolated the results to 24 GeV.

Our order-of-magnitude estimates indicate that many  $T_{cc}$  states, hidden-charm pentaquarks, and hidden-charm baryon-antibaryon states can be produced at EIC. While EicC will have little chance to observe double-charm  $T_{cc}$  states, lots of events can be collected in the study of hidden-charm pentaquarks and certain baryon-antibaryon molecules such as the  $\Lambda_c \bar{\Lambda}_c$  molecular state. In addition, the high



luminosity of the proposed 24 GeV upgrade allows CEBAF to play an important role in the search for the hidden-charm tetraquarks and pentaquarks.

### ACKNOWLEDGMENTS

We are grateful to Jorgivan Morais Dias, Shu-Ming Wu, Mao-Jun Yan, and Zhen-Hua Zhang for useful discussions. The numerical calculations were done at the HPC Cluster of ITP-CAS. This work is supported in part by the Chinese Academy of Sciences under Grant No. XDB34030000; by the National Natural Science Foundation of China (NSFC) under Grants No. 12125507, No. 11835015, No. 12047503, No. 11961141012, and No. 12275046; by the NSFC and

the Deutsche Forschungsgemeinschaft (DFG) through the funds provided to the TRR110 “Symmetries and the Emergence of Structure in QCD” (NSFC Grant No. 12070131001, DFG Project-ID 196253076); and by the Natural Science Foundation of Sichuan Province under Grant No. 2022NSFSC1795.

### APPENDIX: CROSS SECTION FORMULA FOR THE SPIN-3/2 MOLECULE COMPOSED OF A BARYON AND VECTOR MESON

The differential cross section for the inclusive production of a  $BV$  pair in the c.m. frame, where  $B$  and  $V$  denote a baryon with spin  $S = 1/2$  and a vector meson, respectively, is

$$\begin{aligned} d\sigma[\text{all} + BV^*(k)]_{\text{MC}} &= \frac{1}{\text{flux}} \sum_{\text{all}} \int d\phi_{\text{all}+BV} \text{Tr}(\mathcal{M}_i[\text{all} + BV] \bar{u}[B] u[B] \mathcal{M}_j^*[\text{all} + BV]) \epsilon^i[V] \epsilon^{*j}[V] \frac{d^3k}{(2\pi)^3 2\mu} \\ &\simeq 2m_B \frac{1}{\text{flux}} \sum_{\text{all}} \int d\phi_{\text{all}+BV} \text{Tr}(\mathcal{M}^i[\text{all} + BV] \mathcal{M}_i^*[\text{all} + BV]) \frac{d^3k}{(2\pi)^3 2\mu}, \end{aligned} \quad (\text{A1})$$

where  $\epsilon^i[V]$  is the polarization vector of the vector meson  $V$ , and  $u[B]$  is the Dirac spinor of the baryon  $B$ .  $m_B$ ,  $m_V$ , and  $\mu$  are the masses of  $B$  and  $V$  and the reduced mass of the  $BV$  pair, respectively. The cross section for the inclusive production of a  $BV$  molecule with spin  $S = 3/2$ , denoted by  $X_1$ , is

$$\begin{aligned} \sigma[X_1 + \text{all}] &= \frac{1}{\text{flux}} \sum_{\text{all}} \int d\phi_{\text{all}+BV} \text{Tr}\{\mathcal{M}_i[\text{all} + BV] (\not{k}_1 + m_B) \delta^{ii'} 2m_B G_R g_X \bar{u}_{i'}[X_1] \\ &\quad u_j[X_1] g_X \delta^{jj'} (\not{k}_1 + m_B) G_R^* \mathcal{M}_j^*[\text{all} + BV]\} \frac{d^3k}{(2\pi)^3 2\mu} \\ &\simeq \frac{2m_{X_1} 4m_B^2}{16m_V^2 m_B^2} \frac{1}{\text{flux}} \sum_{\text{all}} \int d\phi_{\text{all}+BV} \text{Tr}[\mathcal{M}_j[\text{all} + BV] P^{(3/2)ij} \mathcal{M}_i^*[\text{all} + BV]] |G(E, \Lambda) g_X|^2 \frac{d^3k}{(2\pi)^3 2\mu} \\ &= \frac{2}{3} \frac{m_{X_1}}{2m_V^2} \frac{1}{\text{flux}} \sum_{\text{all}} \int d\phi_{\text{all}+BV} \text{Tr}[\mathcal{M}^i[\text{all} + BV] \mathcal{M}_i^*[\text{all} + BV]] |G(E, \Lambda) g_X|^2 \frac{d^3k}{(2\pi)^3 2\mu} \\ &\simeq \frac{m_{X_1}}{3m_V m_B} |G(E, \Lambda) g_{\text{eff}}|^2 \left( \frac{d\sigma[\text{all} + BV]}{dk} \right)_{\text{MC}} \frac{4\pi^2 \mu}{k^2}, \end{aligned} \quad (\text{A2})$$

where  $G_R$  is the relativistic scalar two-point loop function,  $m_X$  is the mass of  $X_1$ ,  $k_1$  is the four-momentum of the baryon  $B$ ,  $g_{\text{eff}}$  is the effective coupling constant in Eq. (6), and  $G(E, \Lambda)$  is the Green's function in Eq. (5).  $u_i[X_1]$  is the spinor of  $X_1$ , and  $P_{ij}^{(3/2)}$  is the nonrelativistic projection operator of a spin-3/2 particle [84],

$$P_{ij}^{(3/2)} = \frac{2}{3} \delta_{ij} - \frac{i}{3} \epsilon_{ijk} \sigma^k. \quad (\text{A3})$$

Matching Eq. (A2) with the general cross section formula of Eq. (3), one can get  $\mathcal{N} = 2/3$  for the production of  $X_1$ . Using the same method, one can get  $\mathcal{N} = 1$  for the other hadronic molecules discussed in this work.

- [1] M. Ablikim *et al.* (BESIII Collaboration), *Chin. Phys. C* **44**, 040001 (2020).
- [2] A. Cerri *et al.*, *CERN Yellow Rep. Monogr.* **7**, 867 (2019).
- [3] W. Altmannshofer *et al.* (Belle-II Collaboration), *Prog. Theor. Exp. Phys.* **2019**, 123C01 (2019); **2020**, 029201 (E) (2020).
- [4] H.-X. Chen, W. Chen, X. Liu, and S.-L. Zhu, *Phys. Rep.* **639**, 1 (2016).
- [5] A. Hosaka, T. Iijima, K. Miyabayashi, Y. Sakai, and S. Yasui, *Prog. Theor. Exp. Phys.* **2016**, 062C01 (2016).
- [6] R. F. Lebed, R. E. Mitchell, and E. S. Swanson, *Prog. Part. Nucl. Phys.* **93**, 143 (2017).
- [7] A. Esposito, A. Pilloni, and A. D. Polosa, *Phys. Rep.* **668**, 1 (2017).
- [8] F.-K. Guo, C. Hanhart, U.-G. Meißner, Q. Wang, Q. Zhao, and B.-S. Zou, *Rev. Mod. Phys.* **90**, 015004 (2018).
- [9] S. L. Olsen, T. Skwarnicki, and D. Zieminska, *Rev. Mod. Phys.* **90**, 015003 (2018).
- [10] Y.-R. Liu, H.-X. Chen, W. Chen, X. Liu, and S.-L. Zhu, *Prog. Part. Nucl. Phys.* **107**, 237 (2019).
- [11] N. Brambilla, S. Eidelman, C. Hanhart, A. Nefediev, C.-P. Shen, C. E. Thomas, A. Vairo, and C.-Z. Yuan, *Phys. Rep.* **873**, 1 (2020).
- [12] F.-K. Guo, X.-H. Liu, and S. Sakai, *Prog. Part. Nucl. Phys.* **112**, 103757 (2020).
- [13] H.-X. Chen, W. Chen, X. Liu, Y.-R. Liu, and S.-L. Zhu, *arXiv:2204.02649*.
- [14] C. Adolph *et al.* (COMPASS Collaboration), *Phys. Lett. B* **742**, 330 (2015).
- [15] M. Aghasyan *et al.* (COMPASS Collaboration), *Phys. Lett. B* **783**, 334 (2018).
- [16] A. Ali *et al.* (GlueX Collaboration), *Phys. Rev. Lett.* **123**, 072001 (2019).
- [17] D. P. Anderle *et al.*, *Front. Phys. (Beijing)* **16**, 64701 (2021).
- [18] R. Abdul Khalek *et al.*, *Nucl. Phys. A* **1026**, 122447 (2022).
- [19] J. Arrington *et al.*, *Prog. Part. Nucl. Phys.* **127**, 103985 (2022).
- [20] Y. Huang, J. He, H.-F. Zhang, and X.-R. Chen, *J. Phys. G* **41**, 115004 (2014).
- [21] Q. Wang, X.-H. Liu, and Q. Zhao, *Phys. Rev. D* **92**, 034022 (2015).
- [22] Y. Huang, J.-J. Xie, J. He, X. Chen, and H.-F. Zhang, *Chin. Phys. C* **40**, 124104 (2016).
- [23] A. N. Hiller Blin, C. Fernández-Ramírez, A. Jackura, V. Mathieu, V. I. Mokeev, A. Pilloni, and A. P. Szczepaniak, *Phys. Rev. D* **94**, 034002 (2016).
- [24] M. Karliner and J. L. Rosner, *Phys. Lett. B* **752**, 329 (2016).
- [25] V. Kubarovsky and M. B. Voloshin, *Phys. Rev. D* **92**, 031502 (2015).
- [26] D. Winney, C. Fanelli, A. Pilloni, A. N. Hiller Blin, C. Fernández-Ramírez, M. Albaladejo, V. Mathieu, V. I. Mokeev, and A. P. Szczepaniak (JPAC Collaboration), *Phys. Rev. D* **100**, 034019 (2019).
- [27] E. Y. Paryev and Y. T. Kiselev, *Nucl. Phys. A* **978**, 201 (2018).
- [28] X.-Y. Wang, X.-R. Chen, and J. He, *Phys. Rev. D* **99**, 114007 (2019).
- [29] V. P. Gonçalves and M. M. Jaime, *Phys. Lett. B* **805**, 135447 (2020).
- [30] J.-J. Wu, T. S. H. Lee, and B.-S. Zou, *Phys. Rev. C* **100**, 035206 (2019).
- [31] Y.-P. Xie, X. Cao, Y.-T. Liang, and X. Chen, *Chin. Phys. C* **45**, 043105 (2021).
- [32] Z. Yang, X. Cao, Y.-T. Liang, and J.-J. Wu, *Chin. Phys. C* **44**, 084102 (2020).
- [33] X.-H. Liu, Q. Zhao, and F. E. Close, *Phys. Rev. D* **77**, 094005 (2008).
- [34] G. Galata, *Phys. Rev. C* **83**, 065203 (2011).
- [35] Q.-Y. Lin, X. Liu, and H.-S. Xu, *Phys. Rev. D* **88**, 114009 (2013).
- [36] Q.-Y. Lin, X. Liu, and H.-S. Xu, *Phys. Rev. D* **89**, 034016 (2014).
- [37] X.-Y. Wang, X.-R. Chen, and A. Guskov, *Phys. Rev. D* **92**, 094017 (2015).
- [38] M. Albaladejo, A. N. H. Blin, A. Pilloni, D. Winney, C. Fernández-Ramírez, V. Mathieu, and A. Szczepaniak (JPAC Collaboration), *Phys. Rev. D* **102**, 114010 (2020).
- [39] M.-L. Du, V. Baru, F.-K. Guo, C. Hanhart, U.-G. Meißner, A. Nefediev, and I. Strakovsky, *Eur. Phys. J. C* **80**, 1053 (2020).
- [40] Y.-Z. Xu, S. Chen, Z.-Q. Yao, D. Binosi, Z.-F. Cui, and C. D. Roberts, *Eur. Phys. J. C* **81**, 895 (2021).
- [41] Z. Yang and F.-K. Guo, *Chin. Phys. C* **45**, 123101 (2021).
- [42] P. Artoisenet and E. Braaten, *Phys. Rev. D* **83**, 014019 (2011).
- [43] F.-K. Guo, U.-G. Meißner, W. Wang, and Z. Yang, *J. High Energy Phys.* **05** (2014) 138.
- [44] F.-K. Guo, U.-G. Meißner, W. Wang, and Z. Yang, *Eur. Phys. J. C* **74**, 3063 (2014).
- [45] C. Bignamini, B. Grinstein, F. Piccinini, A. D. Polosa, and C. Sabelli, *Phys. Rev. Lett.* **103**, 162001 (2009).
- [46] P. Artoisenet and E. Braaten, *Phys. Rev. D* **81**, 114018 (2010).
- [47] M. Albaladejo, F.-K. Guo, C. Hanhart, U.-G. Meißner, J. Nieves, A. Nogga, and Z. Yang, *Chin. Phys. C* **41**, 121001 (2017).
- [48] F.-K. Guo, U.-G. Meißner, and W. Wang, *Commun. Theor. Phys.* **61**, 354 (2014).
- [49] P. Ling, X.-H. Dai, M.-L. Du, and Q. Wang, *Eur. Phys. J. C* **81**, 819 (2021).
- [50] P.-P. Shi, Z.-H. Zhang, F.-K. Guo, and Z. Yang, *Phys. Rev. D* **105**, 034024 (2022).
- [51] G. Bauer (CDF Collaboration), *Int. J. Mod. Phys. A* **20**, 3765 (2005).
- [52] S. Chatrchyan *et al.* (CMS Collaboration), *J. High Energy Phys.* **04** (2013) 154.
- [53] R. Aaij *et al.* (LHCb Collaboration), *Phys. Rev. Lett.* **122**, 222001 (2019).
- [54] R. Aaij *et al.* (LHCb Collaboration), *Sci. Bull.* **66**, 1278 (2021).
- [55] R. Aaij *et al.* (LHCb Collaboration), *Nat. Commun.* **13**, 3351 (2022).
- [56] R. Aaij *et al.* (LHCb Collaboration), *Nat. Phys.* **18**, 751 (2022).
- [57] S. K. Choi *et al.* (Belle Collaboration), *Phys. Rev. Lett.* **91**, 262001 (2003).
- [58] M. Ablikim *et al.* (BESIII Collaboration), *Phys. Rev. Lett.* **110**, 252001 (2013).

- [59] Z. Q. Liu *et al.* (Belle Collaboration), *Phys. Rev. Lett.* **110**, 252002 (2013); **111**, 019901(E) (2013).
- [60] M. Ablikim *et al.* (BESIII Collaboration), *Phys. Rev. Lett.* **115**, 112003 (2015).
- [61] X.-K. Dong, F.-K. Guo, and B.-S. Zou, *Progr. Phys.* **41**, 65 (2021).
- [62] X.-K. Dong, F.-K. Guo, and B.-S. Zou, *Commun. Theor. Phys.* **73**, 125201 (2021).
- [63] E. Braaten and M. Kusunoki, *Phys. Rev. D* **72**, 014012 (2005).
- [64] T. Sjostrand, S. Mrenna, and P. Z. Skands, *J. High Energy Phys.* **05** (2006) 026.
- [65] J. Nieves and M. P. Valderrama, *Phys. Rev. D* **86**, 056004 (2012).
- [66] F.-K. Guo, C. Hidalgo-Duque, J. Nieves, and M. P. Valderrama, *Phys. Rev. D* **88**, 054007 (2013).
- [67] M.-Z. Liu, Y.-W. Pan, F.-Z. Peng, M. Sánchez Sánchez, L.-S. Geng, A. Hosaka, and M. Pavon Valderrama, *Phys. Rev. Lett.* **122**, 242001 (2019).
- [68] Z. Yang, X. Cao, F.-K. Guo, J. Nieves, and M. P. Valderrama, *Phys. Rev. D* **103**, 074029 (2021).
- [69] R. Aaij *et al.* (LHCb Collaboration), *Phys. Rev. D* **102**, 092005 (2020).
- [70] C. Hanhart, Y. S. Kalashnikova, A. E. Kudryavtsev, and A. V. Nefediev, *Phys. Rev. D* **85**, 011501 (2012).
- [71] C. Hidalgo-Duque, J. Nieves, and M. P. Valderrama, *Phys. Rev. D* **87**, 076006 (2013).
- [72] M. Ablikim *et al.* (BESIII Collaboration), *Phys. Rev. Lett.* **126**, 102001 (2021).
- [73] M.-L. Du, V. Baru, X.-K. Dong, A. Filin, F.-K. Guo, C. Hanhart, A. Nefediev, J. Nieves, and Q. Wang, *Phys. Rev. D* **105**, 014024 (2022).
- [74] M.-Z. Liu, Y.-W. Pan, and L.-S. Geng, *Phys. Rev. D* **103**, 034003 (2021).
- [75] R. Chen, *Phys. Rev. D* **103**, 054007 (2021).
- [76] F.-Z. Peng, M.-J. Yan, M. Sánchez Sánchez, and M. P. Valderrama, *Eur. Phys. J. C* **81**, 666 (2021).
- [77] H.-X. Chen, W. Chen, X. Liu, and X.-H. Liu, *Eur. Phys. J. C* **81**, 409 (2021).
- [78] S. Sakai, H.-J. Jing, and F.-K. Guo, *Phys. Rev. D* **100**, 074007 (2019).
- [79] M.-L. Du, V. Baru, F.-K. Guo, C. Hanhart, U.-G. Meißner, J. A. Oller, and Q. Wang, *Phys. Rev. Lett.* **124**, 072001 (2020).
- [80] M.-L. Du, V. Baru, F.-K. Guo, C. Hanhart, U.-G. Meißner, J. A. Oller, and Q. Wang, *J. High Energy Phys.* **08** (2021) 157.
- [81] M.-L. Du, Z.-H. Guo, and J. A. Oller, *Phys. Rev. D* **104**, 114034 (2021).
- [82] R. Aaij *et al.* (LHCb Collaboration), *Phys. Rev. Lett.* **119**, 112001 (2017).
- [83] R. L. Workman (Particle Data Group), *Prog. Theor. Exp. Phys.* **2022**, 083C01 (2022).
- [84] S. U. Chung, Report No. CERN-71-08, CERN, Geneva, 1971, <http://cds.cern.ch/record/186421>.